

**Cavity-assisted atomic Raman memories beyond the bad cavity limit: Effect of four-wave mixing**

N. G. Veselkova, N. I. Masalaeva, and I. V. Sokolov\*

*Faculty of Physics, St. Petersburg State University, 7/9 Universitetskaya naberezhnaya, St. Petersburg, 199034 Russia*

(Received 30 July 2018; published 9 January 2019)

Quantum memories can be used not only for storage of quantum information but also for a substantial manipulation of ensembles of quantum states. Therefore, the speed of such manipulation and the ability to write and retrieve signals of relatively short duration become important. One approach towards enhancing the performance of a quantum memory is to combine an active medium with an optical cavity. Previous works investigating cavity-enhanced memories concentrated on noise processes in the bad cavity limit, that is, for signals that are much longer than the cavity field lifetime. In this work we investigate four-wave mixing noise that arises from the retrieval of relatively short signals from cavity-assisted memories, thus complementing recent works by other authors. We propose an approach that allows one to account for noise sources of different frequencies and different physical origin by using two-band spectral filtering of the noise sources in the Heisenberg-Langevin picture. We demonstrate that in these spectrally selective memories the sideband atomic noise sources contribute to the four-wave mixing noise on par with the sideband quantized field entering the cavity.

DOI: [10.1103/PhysRevA.99.013814](https://doi.org/10.1103/PhysRevA.99.013814)**I. INTRODUCTION**

Efficient quantum memories for light [1–4] are considered an important component of many schemes of quantum information, such as quantum repeaters, quantum networks, quantum computers, etc. Of particular interest for future applications are the schemes that allow for storage and manipulation of signals with many spatial and/or temporal degrees of freedom. In atomic memories, exploiting cold atomic ensembles as a storage medium, the resources for essentially multimode operation are provided by independent spatial waves (quantum holograms) of the collective spin excitation [5–9] and by time multiplexing [10].

Cavity-enhanced atomic memories implemented experimentally with the use of cold [10–12] and warm [13] atomic ensembles demonstrate good efficiency and fidelity of quantum state manipulation. A cavity enhances coupling between the signal field and storage medium by means of multiple passes of light through the atomic ensemble, thus increasing the cooperativity parameter and the cavity field lifetime. On the other hand, coprocessing in a memory of a time sequence of quantized signals [9,10] within the time interval of effective storage implies shortening the signal's duration. In view of this, it is natural to address the question to what extent one can speed up manipulation of a signal in a sequence, achieving maximal information content for the whole ensemble of the signals. The theoretical estimates [14,15], performed mostly in the bad cavity approximation, have revealed that the memory quantum efficiency close to unity is achievable in this limit.

We have investigated [16] the quantum efficiency of cavity-enhanced atomic Raman memories for signals whose duration is not much larger than the cavity field lifetime, that is, beyond

the bad cavity approximation. The nonstationary amplitude and phase shaping of a control field that yields maximal storage efficiency of a given input signal has been studied [17].

Four-wave mixing noise present in real schemes of the atom-field interaction in atomic memories is commonly recognized as an important factor, able to prevent achieving high memory quality. The four-wave mixing arises when besides the memory  $\Lambda$  scheme there is involved an additional  $\Lambda$  scheme, where the same control field produces, via Raman two-quantum transition, pairs of quanta: the quantized field excitation and the collective spin wave excitation (the spin polariton), in analogy to parametric scattering in the presence of  $\chi^{(2)}$  nonlinearity. The arising spin excitations are involved in the readout process on par with the stored signal and constitute an unwanted noise.

The deleterious effect of four-wave mixing noise on the atomic memories' overall efficiency was investigated for both the single-pass [18–20] and cavity-assisted [13,21] schemes. Prajapati *et al.* [20] proposed to suppress the four-wave mixing noise in a single-pass configuration by introducing a two-quantum Raman absorption channel for sideband light. Spectral filtering of the sideband quantized field, performed by a cavity, also makes it possible to suppress effectively the four-wave mixing noise. The noise suppression using a cavity was demonstrated experimentally [13]. The approach presented in Ref. [21] is based on an explicit description of a quantized sideband noise field as an independent wave, performing round-trips inside the cavity. In this picture, the sideband noise can be tuned to the cavity antiresonance, thus achieving better noise suppression. Detailed theoretical analysis [21] of four-wave mixing noise is focused mainly on atomic memory operation in the bad cavity limit.

We present in our work theoretical research of four-wave mixing noise in cavity-assisted atomic Raman memories,

\*i.sokolov@mail.spbu.ru; sokolov.i.v@gmail.com

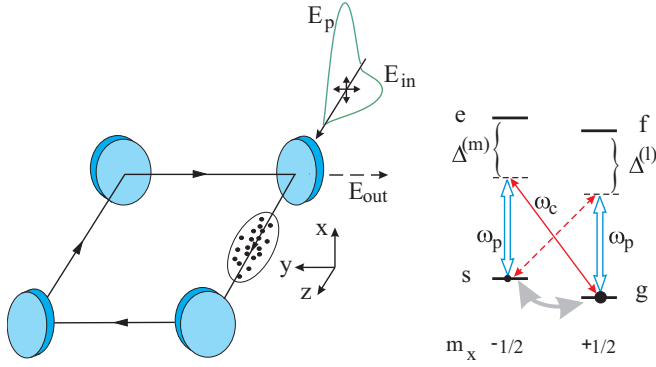


FIG. 1. Raman atomic memory schematic. A control field (double arrows) induces two-quantum Raman transitions in both  $\Lambda$  schemes. A cavity field (solid arrow) and a sideband noise field (dashed arrow) are generated via two-quantum transitions in the memory and luminescence channels, respectively. A signal is stored in the Raman coherence between the lower levels of the scheme (gray arrow).

valid also for signals whose duration is not much longer than the cavity field lifetime, that is, beyond the bad cavity limit. Our generalization may be potentially useful for analysis of essentially multimode regimes of atomic memory operation, where an attainable compromise between the operation speed and the quality of a memory device should be revealed.

Unlike [21], we do not restrict ourselves by considering four-wave mixing noise in the presence of the only noise source that is due to the sideband quantized light field entering the cavity. Our theory is based on two-band spectral filtering of generic noise sources in the Heisenberg-Langevin picture, where the cavity field and the atomic noise sources are treated within the same approach. We demonstrate that in spectrally selective cavity-assisted atomic memories the sideband atomic noise sources essentially contribute to the four-wave mixing noise of the retrieved signal on par with the sideband field entering the cavity.

The finally estimated quantity is the noise variance of quadrature amplitudes of the output signal, observed by means of optimal homodyne detection. We specify and evaluate both analytically and numerically the noise contributions, associated with the four-wave mixing and with the different-from-unity quantum efficiency, for a wide range of the retrieved signal duration, including signals whose duration does not much exceed the cavity field lifetime.

## II. MEMORY CELL IN THE PRESENCE OF FOUR-WAVE MIXING

The memory scheme that will be considered appears in Fig. 1. The Hamiltonian of the electric dipole interaction of  $N$  motionless atoms with the cavity field in the rotating-wave approximation is given by

$$H = H_0 + V,$$

$$H_0 = \hbar\omega_c a^\dagger a + \hbar \sum_{j=1}^N (\omega_{sg} \sigma_{ss}^{(j)} + \omega_{eg} \sigma_{ee}^{(j)} + \omega_{fg} \sigma_{ff}^{(j)}),$$

$$V = -\hbar \sum_{j=1}^N [\Omega^{(m)}(t) \sigma_{es}^{(j)} e^{-i\omega_p t} + \Omega^{(l)}(t) \sigma_{fg}^{(j)} e^{-i\omega_p t} + a g^{(m)} \sigma_{eg}^{(j)} + a g^{(l)} \sigma_{fs}^{(j)}] + \text{H.c.}$$

Here  $a$  is a quantized cavity field which we consider in single-mode approximation, and  $\sigma_{nm}^{(j)} = (|n\rangle\langle m|)^{(j)}$  is the atomic transition operator for the  $j$ th atom, where  $\omega_{nm}$  is the transition frequency. The interaction Hamiltonian written in the Schrödinger picture explicitly depends on a classical control field with Rabi frequency (the slow amplitude)  $\Omega^{(m)}(t)$  and  $\Omega^{(l)}(t)$  in the left and right  $\Lambda$  schemes, respectively. The right one is responsible for the control field Stokes Raman scattering, which results in the generation of bosonic quanta pairs (the light and the collective spin). Having in mind an analogy to parametric generation of pairs in  $\chi^{(2)}$  nonlinear media, we will call the interaction channel, introduced by the right  $\Lambda$  scheme, the Raman luminescence channel (or, for brevity, the luminescence channel).

The cavity frequency  $\omega_c$  and the classical control field frequency  $\omega_p = \omega_c - \omega_{sg}$  are matched in such a way as to support two-quantum resonance in the memory channel, and  $g^{(m)}$  and  $g^{(l)}$  are coupling parameters for the quantized mode field in the corresponding channel.

The single-cavity-mode approximation implies that the frequency mismatch  $2|\omega_{sg}|$  between the memory and luminescence channels is small compared to frequency distance between the cavity modes. Spatial factors are omitted in the Hamiltonian since for the copropagating control and quantized fields the difference between the longitudinal wave numbers  $k_{pz} - k_{cz}$  does not manifest itself in the atomic cloud length. This can be a good approximation for storage within the same hyperfine level. In the case of storage on two different hyperfine levels, the spin polariton might be of an essentially space-dependent form. We do not consider here the spatial addressability resource which allows for an essentially multimode memory operation [9].

The slow amplitudes of the field and the collective atomic observables are introduced as

$$\mathcal{E}(t) = a(t) \exp(i\omega_c t), \quad (1)$$

$$\sigma_{ge}(t) = \sum_{j=1}^N \sigma_{ge}^{(j)}(t) e^{i\omega_c t},$$

$$\sigma_{gs}(t) = \sum_{j=1}^N \sigma_{gs}^{(j)}(t) e^{i\omega_{sg} t}, \quad (2)$$

$$\sigma_{sf}(t) = \sum_{j=1}^N \sigma_{sf}^{(j)}(t) e^{i\omega_c t},$$

$$\sigma_{gf}(t) = \sum_{j=1}^N \sigma_{gf}^{(j)}(t) e^{i(\omega_c + \omega_{sg}) t}. \quad (3)$$

The Heisenberg equations of motion are derived and linearized under the assumption that the ground state  $g$  does not change population within the retrieval cycle,  $\sigma_{gg}^{(j)}(t) \rightarrow 1$ , while the population of all other states as well as the cross

coherences  $\sigma_{es}^{(j)}$  and  $\sigma_{fe}^{(j)}$  can be neglected, with the exception of the polarization  $\sigma_{sf}^{(j)}$ , which couples the cavity field to the luminescence channel.

By introducing the cavity field decay at a rate  $\kappa$  and the atomic coherence relaxation, induced by the upper state decay, at a rate  $\gamma_{\perp}$ , we arrive at

$$\dot{\mathcal{E}}(t) = -\kappa\mathcal{E}(t) + ig^{(m)}\sigma_{ge}(t) + ig^{(l)}\sigma_{sf}(t) + \sqrt{2\kappa}\mathcal{E}_{in}(t), \quad (4)$$

$$\dot{\sigma}_{ge}(t) = -(\gamma_{\perp} + i\Delta^{(m)})\sigma_{ge}(t) + i\Omega^{(m)}(t)\sigma_{gs}(t) + ig^{(m)}N\mathcal{E}(t) + \sqrt{2\gamma_{\perp}N}F_{ge}(t), \quad (5)$$

$$\dot{\sigma}_{gs}(t) = i\Omega^{(m)*}(t)\sigma_{ge}(t) - i\Omega^{(l)}(t)e^{i2\omega_{sg}t}\sigma_{fs}(t) + ig^{(l)}\mathcal{E}^{\dagger}(t)\sigma_{gf}(t), \quad (6)$$

$$\dot{\sigma}_{gf}(t) = -[\gamma_{\perp} + i(\Delta^{(l)} - 2\omega_{sg})]\sigma_{gf}(t) + i\Omega^{(l)}(t)Ne^{i2\omega_{sg}t} + ig^{(l)}\mathcal{E}(t)\sigma_{gs}(t) + \sqrt{2\gamma_{\perp}N}F_{gf}(t), \quad (7)$$

$$\dot{\sigma}_{sf}(t) = -[\gamma_{\perp} + i(\Delta^{(l)} - 2\omega_{sg})]\sigma_{sf}(t) + i\Omega^{(l)}(t)e^{i2\omega_{sg}t}\sigma_{sg}(t) + \sqrt{2\gamma_{\perp}N}F_{sf}(t). \quad (8)$$

The input cavity field  $\mathcal{E}_{in}(t)$  and the Langevin noise operators  $F_{nm}(t)$  (corresponding to vacuum noise fields) satisfy standard commutation relations,

$$[\mathcal{E}_{in}(t), \mathcal{E}_{in}^{\dagger}(t')] = [F_{ge}^{\dagger}(t), F_{ge}^{\dagger}(t')] \\ = [F_{gf}(t), F_{gf}^{\dagger}(t')] = \delta(t - t'), \quad (9)$$

which preserve the commutation relation  $[\mathcal{E}(t), \mathcal{E}^{\dagger}(t)] = 1$  for the cavity field and the properties of atomic observables of the form  $\sigma_{kl}(t)\sigma_{mn}(t) = \delta_{lm}\sigma_{kn}(t)$  (Einstein's theorem). The same assumption of unchanged population of the ground state  $g$  was used when deriving (9). The noise source  $F_{sf}$  has zero power in this limit and will be omitted.

Now we introduce, in analogy to [16,17], physically reasonable corrections to the field and atomic frequencies. The cavity mode frequency shift due to the linear refractive index is

$$\delta_c = -\frac{g^{(m)2}N}{\Delta^{(m)}}. \quad (10)$$

The dynamic correction  $\delta_s(t)$  to the frequency  $\omega_{sg}$  of the  $s$ - $g$  transition due to ac Stark shifts, induced by the strong control field (which might not be mutually compensating in

the general case), results in an additional phase  $\varphi_s(t)$  of the collective spin coherence,  $\sigma_{gs}(t) \sim \exp[-i\varphi_s(t)]$ , where

$$\delta_s(t) = -\left(\frac{|\Omega^{(m)}(t)|^2}{\Delta^{(m)}} - \frac{|\Omega^{(l)}(t)|^2}{\Delta^{(l)}}\right), \\ \varphi_s(t) = \int_0^t dt' \delta_s(t'). \quad (11)$$

These phase corrections are incorporated into a new self-consistent set of slow field and atomic variables,

$$\mathcal{E}(t) = e^{-i\delta_c t} \tilde{\mathcal{E}}(t), \quad \mathcal{E}_{in}(t) = e^{-i\delta_c t} \tilde{\mathcal{E}}_{in}(t), \quad (12)$$

$$\sigma_{ge}(t) = e^{-i\delta_c t} \tilde{\sigma}_{ge}(t), \quad \sigma_{gs}(t) = e^{-i\varphi_s(t)} \tilde{\sigma}_{gs}(t), \quad (13)$$

$$\sigma_{gf}(t) = e^{-i[\delta_c t + \varphi_s(t)]} \tilde{\sigma}_{gf}(t), \quad \sigma_{sf}(t) = e^{-i\delta_c t} \tilde{\sigma}_{sf}(t), \quad (14)$$

$$\Omega^{(m)}(t) = e^{-i(\delta_c t - \varphi_s(t))} \tilde{\Omega}^{(m)}(t), \\ \Omega^{(l)}(t) = e^{-i[\delta_c t - \varphi_s(t)]} \tilde{\Omega}^{(l)}(t). \quad (15)$$

New noise operators are defined similarly to the corresponding atomic variables.

Next, we substitute these definitions in the basic equations above and perform the first adiabatic elimination. That is, we assume the Raman regime condition when both frequency mismatches  $|\Delta^{(m)}|$  and  $|\Delta^{(l)}|$  are much larger than other frequency parameters of the scheme. The quantities  $(d/dt)\tilde{\sigma}_{ge}$ ,  $(d/dt)\tilde{\sigma}_{gf}$ , and  $(d/dt)\tilde{\sigma}_{sf}$  are set to zero; the corresponding observables are expressed in terms of other variables and substituted into the remaining equations. In the following, we drop the tildes for brevity and use the notation  $S(t)$  for bosonic collective spin amplitude,  $S(t) = \sigma_{gs}(t)/\sqrt{N}$ , for compatibility with other papers.

To avoid exceeding the accuracy, we omit the spin transition frequency  $\omega_{sg}$  and frequency corrections  $\delta_c$  and  $\delta_s(t)$  when they come in the sum with large Raman mismatches and neglect the terms of order higher than 1 in  $\gamma_{\perp}/|\Delta^{(m)}| \ll 1$  in the resulting equations.

Another important assumption is the large enough frequency mismatch  $2\omega_{sg}$  between the field frequencies that are supported by the Raman two-quantum transitions in the memory and luminescence channels,  $2|\omega_{sg}| \gg \gamma_{\perp}, \kappa$  (see Fig. 1). This implies a weak coupling of the memory to the luminescence channel and makes it possible to consider the terms responsible for the interplay between the two channels in the lowest (zeroth) approximation in  $\gamma_{\perp}/|\Delta^{(l)}| \ll 1$ . We arrive at

$$\dot{\mathcal{E}}(t) = -\left[\kappa + \frac{g^{(m)2}N\gamma_{\perp}}{\Delta^{(m)2}}\right]\mathcal{E}(t) + \frac{ig^{(m)}\sqrt{N}}{\Delta^{(m)}}\left(1 + \frac{i\gamma_{\perp}}{\Delta^{(m)}}\right)\Omega^{(m)}(t)S(t) + \frac{ig^{(l)}\sqrt{N}}{\Delta^{(l)}}\Omega^{(l)}(t)e^{i2(\omega_{sg}t + \varphi_s(t))}S^{\dagger}(t) + \sqrt{2\kappa}\mathcal{E}_{in}(t) + F_{\mathcal{E}}(t), \quad (16)$$

$$\dot{S}(t) = -\gamma_{\perp}\left(\frac{|\Omega^{(m)}(t)|^2}{\Delta^{(m)2}} + \frac{|\Omega^{(l)}(t)|^2}{\Delta^{(l)2}}\right)S(t) + \frac{ig^{(m)}\sqrt{N}}{\Delta^{(m)}}\left(1 + \frac{i\gamma_{\perp}}{\Delta^{(m)}}\right)\Omega^{(m)*}(t)\mathcal{E}(t) + \frac{ig^{(l)}\sqrt{N}}{\Delta^{(l)}}\Omega^{(l)}(t)e^{i2[\omega_{sg}t + \varphi_s(t)]}\mathcal{E}^{\dagger}(t) + F_S(t). \quad (17)$$

One can observe here the terms oscillating at the frequency  $2[\omega_{sg} + \delta_s(t)]$ , which is the frequency detuning of the Raman Stokes transition in the right  $\Lambda$  scheme from resonance with the cavity. These terms are due to the luminescence channel and are able to introduce some squeezing and entanglement to the memory operation, as we demonstrate below. The ground state  $g$  excitation by the control field in the right  $\Lambda$  scheme results in additional relaxation of the spin amplitude at the rate  $\gamma_{\perp}|\Omega^{(l)}|^2/\Delta^{(l)2}$  in Eq. (17), where the factor  $\sim\gamma_{\perp}/\Delta^{(l)2}$  represents off-resonant spectral density of the  $g$ - $f$  line.

The Langevin sources  $F_{\mathcal{E}}$  and  $F_S$  on the right-hand side of (16) and (17) are linear combinations of the previously defined atomic sources. Applying the same approximations, we obtain

$$F_{\mathcal{E}}(t) = \frac{g^{(m)}\sqrt{2\gamma_{\perp}N}}{\Delta^{(m)}}F_{ge}(t), \quad (18)$$

$$F_S(t) = \Omega^{(m)*}(t)\frac{\sqrt{2\gamma_{\perp}}}{\Delta^{(m)}}F_{ge}(t) + g^{(l)}\mathcal{E}^{\dagger}(t)\frac{\sqrt{2\gamma_{\perp}}}{\Delta^{(l)}}F_{gf}(t). \quad (19)$$

Considering a weak (compared to the control field) quantized signal,  $g^{(l)2}\langle\mathcal{E}^{\dagger}\mathcal{E}\rangle \ll |\Omega^{(m)}|^2$ , we neglect the term  $\sim F_{gf}$  in Eq. (19). To be more specific, we restrict ourselves to the case when both  $\Lambda$  schemes are based on the same set of hyperfine levels and assume  $g^{(m)} = g^{(l)} = g$ ,  $\Omega^{(m)}(t) = \Omega^{(l)}(t) = \Omega(t)$ . Since the single-photon detuning is much larger than the energy difference  $\omega_{sg}$  between the two storage states, we also assume  $\Delta^{(m)} = \Delta^{(l)} = \Delta$ .

### III. SPECTRAL FILTERING

In this section, we introduce two-band representation for both the noise sources and the observables. This allows us to take into account the sideband atomic noise sources on par with the sideband quantized noise field entering the cavity.

The second adiabatic elimination is performed under the assumption that the frequency mismatch  $2\omega_{sg}$  is much larger than all other frequencylike coefficients in Eqs. (16) and (17), that is, much larger than the decay rates of the field and spin amplitudes and the field-spin coupling due to the Raman transitions  $g$ - $e$ - $s$  and  $g$ - $f$ - $s$ . Given that  $|\omega_{sg}| \gg |\delta_s(t)|$ , we introduce new slow amplitudes  $\mathcal{E}^{(n)}$  and  $S^{(n)}$ ,  $n = m, l$ , which represent the observables' evolution in two nonoverlapping frequency bands associated with the memory and luminescence channels,

$$\begin{aligned} \mathcal{E}(t) &= \mathcal{E}^{(m)}(t) + \mathcal{E}^{(l)}(t)e^{i2\omega_{sg}t}, \\ S(t) &= S^{(m)}(t) + S^{(l)}(t)e^{i2\omega_{sg}t}. \end{aligned} \quad (20)$$

A similar representation is assumed for the noise operators  $F_n(t)$ ,  $n = \mathcal{E}, S$ , and the input field  $\mathcal{E}_{\text{in}}(t)$ ,

$$\begin{aligned} \mathcal{E}_{\text{in}}(t) &= \mathcal{E}_{\text{in}}^{(m)}(t) + \mathcal{E}_{\text{in}}^{(l)}(t)e^{i2\omega_{sg}t}, \\ F_n(t) &= F_n^{(m)}(t) + F_n^{(l)}(t)e^{i2\omega_{sg}t}. \end{aligned} \quad (21)$$

In order to define the latterly introduced quantities  $F_n^{(m)}(t)$  and  $F_n^{(l)}(t)$ , one has to perform spectral filtering of the initial noise sources (18) and (19) by multiplying their Fourier transforms by two nonoverlapping filtering functions:  $\Pi^{(m)}(\omega)$ , centered at  $\omega = 0$ , and  $\Pi^{(l)}(\omega)$ , centered at  $\omega = -2\omega_{sg}$ . The filtering functions have a width of  $\sim|\omega_{sg}|$  and do not attenuate

Fourier amplitudes within their width. Hence, the correlation time of the filtered noise sources is of the order of  $|\omega_{sg}|^{-1}$ . If the initial sources satisfy the relation

$$[F_n(t), F_m^{\dagger}(t')] = A_{nm}(t)\delta(t-t'), \quad n, m = \mathcal{E}, S, \quad (22)$$

where  $A_{nm}$  is noise covariance power, we arrive after some calculations at

$$\begin{aligned} [F_n^{(i)}(t), F_m^{(j)\dagger}(t')] &= \delta_{ij}A_{nm}(t)\tilde{\delta}(t-t'), \\ i, j &= m, l, \quad n, m = \mathcal{E}, S. \end{aligned} \quad (23)$$

The deltalike function  $\tilde{\delta}(t-t')$  has a temporal width of  $\sim|\omega_{sg}|^{-1}$ . The filtered noise amplitudes in these two channels are mutually independent and are ‘‘slow’’ in terms of the first adiabatic elimination but can be viewed as ‘‘fast’’ compared to the observables  $\mathcal{E}^{(i)}(t)$  and  $S^{(i)}(t)$ ,  $i = m, l$ . The same holds true for the input field.

The definitions (20) and (21) are substituted into the evolution equations (16) and (17). Omitting fast oscillating terms, we arrive at the equations for slow amplitudes  $\mathcal{E}^{(i)}(t)$  and  $S^{(i)}(t)$ ,  $i = m, l$ . The observables related to the luminescence channel are expressed in terms of those for the memory channel by means of adiabatic elimination; that is,  $\dot{\mathcal{E}}^{(l)}$  and  $\dot{S}^{(l)}$  are set to zero compared to  $2\omega_{sg}\mathcal{E}^{(l)}$  and  $2\omega_{sg}S^{(l)}$ . This yields

$$\begin{aligned} \dot{\mathcal{E}}^{(m)}(t) &= -\left[\left(\kappa + \frac{g^2N\gamma_{\perp}}{\Delta^2}\right) + i\delta_R(t)\right]\mathcal{E}^{(m)}(t) \\ &\quad + \frac{ig\sqrt{N}}{\Delta}\left(1 + \frac{i\gamma_{\perp}}{\Delta}\right)\Omega(t)S^{(m)}(t) + \Phi_{\mathcal{E}}(t), \end{aligned} \quad (24)$$

$$\begin{aligned} \dot{S}^{(m)}(t) &= -\left[2\frac{\gamma_{\perp}|\Omega(t)|^2}{\Delta^2} + i\delta_R(t)\right]S^{(m)}(t) \\ &\quad + \frac{ig\sqrt{N}}{\Delta}\left(1 + \frac{i\gamma_{\perp}}{\Delta}\right)\Omega^*(t)\mathcal{E}^{(m)}(t) + \Phi_S(t). \end{aligned} \quad (25)$$

Here

$$\delta_R(t) = -\frac{g^2N|\Omega(t)|^2}{2\omega_{sg}\Delta^2}$$

is the frequency correction induced by the Raman two-quantum transition in the right  $\Lambda$  scheme. This frequency correction is of the order of  $|\delta_c\delta_s/\omega_{sg}| \ll |\delta_c|, |\delta_s|$  and will be omitted due to our approximations. The label  $(m)$  on the observables of interest  $\mathcal{E}^{(m)}$  and  $S^{(m)}$  will be dropped for brevity.

Combined Langevin noise operators in Eqs. (24) and (25) arise in the form

$$\Phi_{\mathcal{E}}(t) = -\frac{g\sqrt{N}}{2\omega_{sg}\Delta}\Omega(t)F_S^{(l)\dagger}(t) + F_{\mathcal{E}}^{(m)}(t) + \sqrt{2\kappa}\mathcal{E}_{\text{in}}^{(m)}(t), \quad (26)$$

$$\Phi_S(t) = -\frac{g\sqrt{N}}{2\omega_{sg}\Delta}\Omega(t)[F_{\mathcal{E}}^{(l)\dagger}(t) + \sqrt{2\kappa}\mathcal{E}_{\text{in}}^{(l)\dagger}(t)] + F_S^{(m)}(t). \quad (27)$$

Coupling the luminescence channel to the memory scheme leads to the following:

(i) The spin amplitude damping rate increases due to excitation of the initial state  $g$  by the control field in the spectral wing of the  $g$ - $f$  transition [see (17) and (25)]. This has some impact on the memory efficiency through the excitations balance (see below).

(ii) New noise terms  $\sim F_n^{(l)\dagger}(t)$ ,  $n = \mathcal{E}, S$ , and the term  $\sim \mathcal{E}_{in}^{(l)\dagger}(t)$  occur in Eqs. (24) and (25) which are responsible for the creation of the field and spin quanta pairs, in analogy to many parametric phenomena. In these noise terms, the atomic noise is represented on par with the noise filed entering the cavity.

In the next sections, we demonstrate that these terms introduce, via four-wave mixing, some additional noise to the memory readout signal, as well as some entanglement of the signal with the spin subsystem.

#### IV. MEMORY READOUT: QUANTUM EFFICIENCY AND NOISE

The output quantized field amplitude is given by the standard input-output relation,

$$\mathcal{E}_{\text{out}}(t) = \sqrt{2\kappa} \mathcal{E}(t) - \mathcal{E}_{\text{in}}(t), \quad (28)$$

which is valid for a high-finesse cavity with a close-to-unity reflection of the cavity mirrors. This very cavity can be viewed as “good” or “bad” depending on how long or short the signal is compared to the cavity lifetime. By the homodyne detection of the output signal on a time interval  $[0, T]$ , the observed quantity is given by the projection of the signal on the normalized homodyne mode  $\mathcal{E}^{(h)}(t) = \sqrt{2\kappa} e^{i\theta_h} \mathcal{E}_0(t)$ ,

$$\frac{n_-}{\langle n \rangle} = \text{Re}(e^{-i\theta_h} \mathcal{E}_d), \quad \mathcal{E}_d = \sqrt{2\kappa} \int_0^T dt \mathcal{E}_{\text{out}}(t) \mathcal{E}_0^*(t), \quad (29)$$

where  $n_-$  and  $\langle n \rangle$  are the difference and the average sum of counts in the arms of the detector and

$$2\kappa \int_0^T dt |\mathcal{E}_0(t)|^2 = 1.$$

The commutation relation (9) implies that the introduced amplitude  $\mathcal{E}_d$  of the output signal temporal mode is bosonic,  $[\mathcal{E}_d, \mathcal{E}_d^\dagger] = 1$ . The directly measured quantity is an arbitrary quadrature component  $\text{Re}(e^{-i\theta_h} \mathcal{E}_d) \equiv Q_h$  of  $\mathcal{E}_d$ , which depends on the homodyne phase  $\theta_h$ . In order to find the signal, we represent the solution of the linear basic equations (24) and (25) in terms of dimensionless Green's functions  $G_{nm}(t, t')$ ,  $n, m = \mathcal{E}, S$ ,

$$\mathcal{E}(t) = G_{\mathcal{E}\mathcal{E}}(t, 0)\mathcal{E}(0) + G_{\mathcal{E}S}(t, 0)S(0) + \int_0^t dt' \sum_{n=\mathcal{E}, S} G_{\mathcal{E}n}(t, t')\Phi_n(t'), \quad (30)$$

$$S(t) = G_{S\mathcal{E}}(t, 0)\mathcal{E}(0) + G_{SS}(t, 0)S(0) + \int_0^t dt' \sum_{n=\mathcal{E}, S} G_{Sn}(t, t')\Phi_n(t'). \quad (31)$$

Consider the memory retrieval. The starting spin amplitude  $S(0)$  is most efficiently transferred to  $\mathcal{E}_d$  given  $\mathcal{E}_{\text{out}}(t) \sim$

$\sqrt{\eta}\sqrt{2\kappa}\mathcal{E}_0(t)S(0)$  when the projection (29) is maximized. In view of (28) and (30), this is achieved when

$$G_{\mathcal{E}S}(t, 0) = \sqrt{\eta}e^{i\theta_R}\mathcal{E}_0(t), \quad (32)$$

where  $\eta \leq 1$  is the quantum efficiency of the readout and  $\theta_R$  is an arbitrary phase shift.

Assuming  $G_{\mathcal{E}S}$  is of the form given by (32) (see the next sections), the observable is found to be

$$\begin{aligned} \mathcal{E}_d &= \sqrt{\eta}e^{i\theta_R}S(0) \\ &+ 2\kappa \int_0^T dt \mathcal{E}_0^*(t) \left( G_{\mathcal{E}\mathcal{E}}(t, 0)\mathcal{E}(0) - \frac{1}{\sqrt{2\kappa}}\mathcal{E}_{\text{in}}^{(m)}(t) \right) \\ &+ 2\kappa \int_0^T dt \mathcal{E}_0^*(t) \int_0^t dt' \sum_{n=\mathcal{E}, S} G_{\mathcal{E}n}(t, t')\Phi_n(t'). \end{aligned} \quad (33)$$

Let us represent a general solution for the signal and spin amplitudes as

$$\mathcal{E}_d = G_{d\mathcal{E}}\mathcal{E}(0) + \sqrt{\eta}e^{i\theta_R}S(0) + G_{d+}\Phi_d^{(+)} + G_{d-}\Phi_d^{(-)}, \quad (34)$$

$$S = G_{S\mathcal{E}}\mathcal{E}(0) + G_{SS}S(0) + G_{S+}\Phi_S^{(+)} + G_{S-}\Phi_S^{(-)}, \quad (35)$$

where we simplified the notation  $S(T) \rightarrow S$ ,  $G_{S\mathcal{E}}(T, 0) \rightarrow G_{S\mathcal{E}}$ ,  $G_{SS}(T, 0) \rightarrow G_{SS}$ .

The terms  $\sim \Phi_d^{(+)}$  and  $\Phi_S^{(+)}$  include the positive-frequency (that is, the annihilation) noise operators, which, as seen from (26) and (27), are associated with the memory channel. The terms  $\sim \Phi_d^{(-)}$  and  $\Phi_S^{(-)}$  are composed of the negative-frequency noise operators, which are introduced by the luminescence channel. We assume that, by definition,

$$\begin{aligned} [\Phi_d^{(+)}, \Phi_d^{(+)\dagger}] &= [\Phi_d^{(-)\dagger}, \Phi_d^{(-)}] \\ &= [\Phi_S^{(+)}, \Phi_S^{(+)\dagger}] = [\Phi_S^{(-)\dagger}, \Phi_S^{(-)}] = 1. \end{aligned} \quad (36)$$

In order to preserve proper commutation relations for the bosonic amplitudes  $\mathcal{E}_d$  and  $S$ , the Green's functions in Eqs. (34) and (35) must obey the following relations:

$$[\mathcal{E}_d, \mathcal{E}_d^\dagger] = |G_{d\mathcal{E}}|^2 + \eta + |G_{d+}|^2 - |G_{d-}|^2 = 1, \quad (37)$$

$$[S, S^\dagger] = |G_{S\mathcal{E}}|^2 + |G_{SS}|^2 + |G_{S+}|^2 - |G_{S-}|^2 = 1, \quad (38)$$

$$\begin{aligned} [\mathcal{E}_d, S^\dagger] &= G_{d\mathcal{E}}G_{S\mathcal{E}}^* + \sqrt{\eta}e^{i\theta_R}G_{SS}^* + G_{d+}G_{S+}^*[\Phi_d^{(+)}, \Phi_S^{(+)\dagger}] \\ &- G_{d-}G_{S-}^*[\Phi_S^{(-)\dagger}, \Phi_d^{(-)}] = 0. \end{aligned} \quad (39)$$

By the memory readout, only the initial spin is assumed to be in a nonvacuum state. For the fluctuation of the observable  $\mathcal{E}_d$  this yields

$$\begin{aligned} \Delta\mathcal{E}_d &= \mathcal{E}_d - \langle \mathcal{E}_d \rangle = \sqrt{\eta}e^{i\theta_R}[S(0) - \langle S(0) \rangle] + G_{d\mathcal{E}}\mathcal{E}(0) \\ &+ G_{d+}\Phi_d^{(+)} + G_{d-}\Phi_d^{(-)}. \end{aligned}$$

The uncertainty of an arbitrary quadrature amplitude of  $\mathcal{E}_d$  is evaluated as  $\langle (\Delta Q_d)^2 \rangle^{1/2}$ , where  $\Delta Q_d = \text{Re}[e^{-i\theta_h} \Delta\mathcal{E}_d]$ . By

making use of (36) and (37), we arrive at

$$\begin{aligned} \langle (\Delta Q_d)^2 \rangle &= \frac{1}{4} \{ 1 + \eta \langle [e^{i(\theta_R - \theta_h)} \Delta S(0) + \text{H.c.}]^2 \rangle : \} \\ &\quad + 2|G_{d-}|^2, \end{aligned} \quad (40)$$

where  $: \cdot :$  denotes normal ordering.

The fluctuation variance (40) is composed of the contributions of (i) an excess over the vacuum level fluctuation of the relevant quadrature of the initial spin, which is transferred to the output with quantum efficiency  $\eta$ , and (ii) the four-wave mixing noise due to the presence of the luminescence channel. By the retrieval of the initial spin in the vacuum state in the absence of luminescence, the output is also in the vacuum state, as it should be.

The added noise, which characterizes the memory device, is found after the removal of the retrieved spin quadrature variance,

$$\begin{aligned} \langle (\Delta Q_d)^2 \rangle^{(\text{add})} &= \langle (\Delta Q_d)^2 \rangle - \eta \langle \{\text{Re}[e^{i(\theta_R - \theta_h)} \Delta S(0)]\}^2 \rangle \\ &= \frac{1}{4} \{ 1 - \eta + 2|G_{d-}|^2 \}. \end{aligned} \quad (41)$$

This is our general result. Further, we will evaluate the impact of both the incomplete readout and the four-wave mixing noise for the values of physical parameters typical for some experiments using cells with alkaline atoms.

## V. OPTIMAL CONTROL OF THE MEMORY CELL

Our goal is to evaluate the added noise (41) for a reasonable range of physical parameters of the memory, that is, to find the readout quantum efficiency  $\eta$ , and to estimate the four-wave mixing noise contribution  $\sim |G_{d-}|^2$ .

The approaches allowing for optimal memory control during the readout, such that the retrieved signal has a predefined temporal shape and satisfies (32), were discussed previously in the literature [14,15,22]. Here we shall use the version of the impedance-matching method presented in Ref. [17], where Raman memory operation beyond the bad cavity limit (that is, for the output signals whose duration is not arbitrarily long compared to the cavity lifetime) was considered in detail. In particular, relaxation phenomena and optimal phase matching of the signal and the control field are addressed.

Since the quantum efficiency  $\eta$  arises as a parameter of the Green's function (32), it can be found by addressing a semiclassical version of the basic equations (24) and (25) and of the input-output relation (28), where the noise sources are dropped. The retrieved signal temporal mode  $\mathcal{E}_0(t)$  is assumed to have a normalized quasi-Gaussian shape of duration  $T$ ,

$$\begin{aligned} \mathcal{E}_0(t) &= N_{\mathcal{E}} \{ \exp[-16(t/T - 1/2)^2] - e^{-4} \}, \\ 2\kappa \int_0^T dt \mathcal{E}_0^2(t) &= 1, \end{aligned} \quad (42)$$

where  $N_{\mathcal{E}}$  is the normalization coefficient. The signal is truncated at the relative level  $1/e^4 \sim 0.018$  and has a width at the relative level  $\sim 1/e$ , equal to half of its duration. The ‘‘inverse’’ problem of estimating the control field time profile  $\Omega(t)$  that matches the predefined time profile of the retrieved signal beyond the bad cavity limit was considered in detail in Ref. [17], where the luminescence channel was not accounted for. This channel introduces to the semiclassical equations

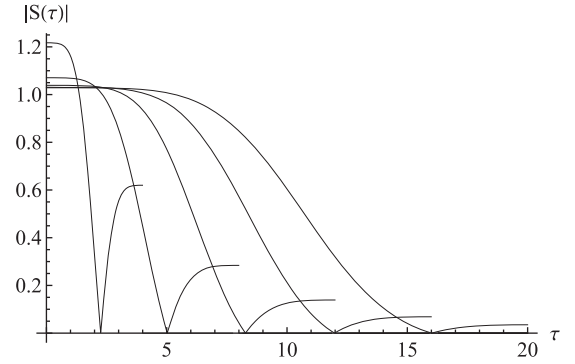


FIG. 2. The spin amplitude for the normalized retrieved signal  $\mathcal{E}_0(t)$  of duration  $2\kappa T = 4, 8, 12, 16, 20$  (in units of the cavity excitation lifetime). At some time moments  $t_s$ , the collective spin excitation is completely mapped onto the cavity field, and the inverse process of the cavity field reabsorption begins in order to shape properly the rear slope of the signal. The shorter the signal is, the larger the fraction of initial atomic excitation is reabsorbed by the memory cell, thus reducing the memory quantum efficiency.

only an additional decay rate of the spin amplitude [see (17) and (25)]. This does not change the basic lines of the consideration given in Ref. [17], and we refer the reader to the cited paper. In brief, the main steps and issues arising are reduced to the following.

The time dependence of the spin excitation number that matches the time profile of the cavity field defined in Eq. (42) is found by integrating the excitation balance,

$$\frac{d}{dt} (|\mathcal{E}_0|^2 + |S|^2) \approx -2 \left( \kappa + \frac{g^2 N \gamma_{\perp}}{\Delta^2} \right) |\mathcal{E}_0|^2 - 4 \frac{\gamma_{\perp} |\Omega S|^2}{\Delta^2}, \quad (43)$$

where  $\Omega S$  is derived from (24),

$$\Omega S \approx \frac{\Delta}{g\sqrt{N}} \left( 1 - i \frac{\gamma_{\perp}}{\Delta} \right) \left[ \frac{d}{dt} + \left( \kappa + \frac{g^2 N \gamma_{\perp}}{\Delta^2} \right) \right] \mathcal{E}_0. \quad (44)$$

Substituting the last expression into (25), one can finally calculate the spin phase,

$$\begin{aligned} \phi_s(t) &= -\frac{\gamma_{\perp}}{\Delta} \int_0^t dt' \frac{1}{|S(t')|^2} \\ &\quad \times \left[ \frac{d}{dt'} + 2 \left( \kappa + \frac{g^2 N \gamma_{\perp}}{\Delta^2} \right) \right] \mathcal{E}_0^2(t'), \end{aligned} \quad (45)$$

where  $S(t) = |S(t)|e^{i\phi_s(t)}$ .

Given the complex spin amplitude evolution is revealed, both the absolute value and the phase of the control field are in turn found by making use of (44).

An essential feature of the memory operation beyond the bad cavity limit, revealed in Ref. [17], is that the rear slope of a signal of a signal of finite duration can be formed only by means of a partial reabsorption of the field excitations by the atomic subsystem, as illustrated in Fig. 2. The reason for this is that free decay of the cavity field after some time moment  $t_s$  would lead to an exponential form of the rear slope of the signal, instead of that of  $\mathcal{E}_0(t)$ . This imposes limitations on quantum efficiency and has some impact on the phase

properties of the system observables. An approach allowing us to regularize the arising nonstationary phase corrections was developed in Ref. [17]. In order to simplify the evaluation of four-wave mixing noise, we neglect here these phase corrections for the signal and the control field in some vicinity of  $t_s$  and take (42) for the signal shape.

The Green's functions of the semiclassical version of (24) and (25) are found by numerical integration, where we make use of the complex control field amplitude calculated in the approach described above. Let us introduce the projections of the Green's functions on the signal temporal mode,

$$\begin{aligned} P_{d\varepsilon}(T, t) &= 2\kappa \int_1^T dt' \mathcal{E}_0^*(t') G_{\varepsilon\varepsilon}(t', t), \\ P_{dS}(T, t) &= 2\kappa \int_1^T dt' \mathcal{E}_0^*(t') G_{\varepsilon S}(t', t). \end{aligned} \quad (46)$$

This yields for the four-wave mixing contribution to the added noise variance (41)

$$\begin{aligned} |G_{d-}|^2 &= \frac{g^2 N}{(2\omega_{sg} \Delta)^2} \int_0^T dt |\Omega(t)|^2 \left\{ |P_{d\varepsilon}(T, t)|^2 \frac{2\gamma_{\perp} |\Omega(t)|^2}{\Delta^2} \right. \\ &+ \left[ P_{d\varepsilon}(T, t) P_{dS}^*(T, t) \frac{2\gamma_{\perp} g \sqrt{N} \Omega(t)}{\Delta^2} + \text{c.c.} \right] \\ &+ |P_{dS}(T, t)|^2 \left( \frac{2\gamma_{\perp} g^2 N}{\Delta^2} + 2\kappa \right) \left. \right\}. \end{aligned} \quad (47)$$

It is common to characterize the atom-field coupling with the cooperativity parameter  $C = g^2 N / \gamma_{\perp} \kappa$  [14]. In our numerical simulation, we assume the following values of the physical parameters corresponding to the off-resonant Raman regime:  $C = 200$ ,  $\gamma_{\perp} / 2\pi = 3$  MHz,  $\kappa / 2\pi = 2$  MHz,  $\Delta / 2\pi = 200$  MHz, and  $\omega_{sg} / 2\pi = 10$  MHz. The dimensionless time  $\tau$  is measured in units of the cavity excitation lifetime  $1/2\kappa$ , where  $\tau = 2\kappa t$ ,  $T = 2\kappa T$ .

We represent the retrieved signal noise (41) by plotting the variance  $4\langle(\Delta Q_d)^2\rangle^{(\text{add})}$  (see curve 1 in Fig. 3). In order to reveal the role of nonadiabatic effects that arise from the memory operation beyond the bad cavity limit, we present our results for a wide range of the signal duration, starting from the relatively short pulses in the timescale of  $1/2\kappa$ , which is beyond the bad cavity limit.

The vacuum noise contribution  $(1 - \eta)$  appears in curve 2, where the memory readout quantum efficiency was derived from the solution of the excitation balance equation (43) as  $\eta = 1/|S(0)|^2$ . Note that in order to retrieve a single excitation from the memory by  $\eta < 1$ , the initial number of spin excitations must exceed 1.

As we demonstrated previously [16,17], the quantum efficiency decrease is basically due to the number of spin excitations  $|S(T)|^2$  retained in the memory by an incomplete readout and to the field and spin relaxation terms in Eqs. (24) and (25), proportional to  $\gamma_{\perp}$ . By the adopted values of the system parameters, just a steep increase in the number of unread excitations for short signals is the main limiting factor for the memory quantum efficiency in the essentially nonadiabatic regime.

The noise term  $2|G_{d-}|^2$  introduced by the four-wave mixing is shown in curve 3. This noise contribution does

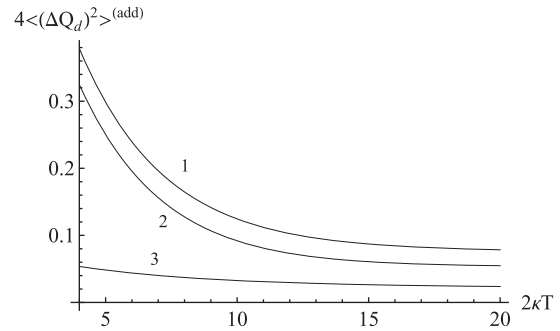


FIG. 3. The added noise variance  $4\langle(\Delta Q_d)^2\rangle^{(\text{add})}$  (curve 1) and the contributions  $1 - \eta$  (curve 2) and  $2|G_{d-}|^2$  (curve 3), associated with the different-from-unity retrieval quantum efficiency  $\eta$  and with the four-wave mixing noise, respectively. As we have demonstrated, the four-wave mixing term stems from both the quantized field and the atomic noise sources. The added noise variance exhibits a significant increase for short signals, especially the contribution  $1 - \eta$ , which is sensitive to a partial signal field reabsorption beyond the bad cavity limit, as illustrated in Fig. 2. In the bad cavity limit (actually for  $2\kappa T > 15, \dots, 20$ ), the quantum efficiency is limited by the excitation of lower atomic sublevels by the control field and by the cavity field absorption.

not demonstrate a comparably significant increase for short signals. An important feature of this source of the memories' imperfection is that for a large enough frequency mismatch  $\omega_{sg}$  this term scales as  $1/\omega_{sg}^2$ , which follows from (47).

## VI. CONCLUSION

We have extended the theory of cavity-assisted atomic Raman memories in the presence of four-wave mixing noise. We have considered the limitations imposed by the four-wave mixing noise and by the noise sources that are due to atomic relaxation for the signals whose duration is not much larger than the cavity field lifetime, that is, beyond the bad cavity limit. Coprocessing in a memory of a time sequence of quantized signals within the time interval of effective storage implies shortening of the signal duration, and our results could help to answer the question of how to achieve maximal information content by reducing the duration of individual signals.

We have proposed an approach that allows one to account for sideband quantum noise sources of different physical origins in cavity-assisted atomic Raman memories using two-band spectral filtering of the noise sources in the Heisenberg-Langevin picture. This allowed us to demonstrate that, in such spectrally selective memories, the sideband atomic noise sources essentially contribute to the four-wave mixing noise of the retrieved signal on par with the sideband quantized field entering the cavity.

## ACKNOWLEDGMENTS

This research was supported by the Russian Foundation for Basic Research (RU) under the projects 16-02-00180-a, 18-02-00648-a, and 19-02-00204-a. NIM acknowledges the RFBR (RU) grant for young researchers 18-32-00255-mol-a.

### APPENDIX A: SPIN NOISE AND ENTANGLEMENT

In order to make our consideration more comprehensive, we briefly review here the statistics of the residual spin excitation  $S(\mathcal{T}) = S$ , as well as its entanglement with the retrieved signal. Equation (35) yields for the spin fluctuation

$$\Delta S = G_{SS}[S(0) - \langle S(0) \rangle] + G_{S\mathcal{E}}\mathcal{E}(0) + G_{S+}\Phi_S^{(+)} + G_{S-}\Phi_S^{(-)}. \quad (\text{A1})$$

The variance of an arbitrary spin fluctuation quadrature  $\Delta Q_S = \text{Re}(e^{-i\theta_S}\Delta S)$  specified by the phase  $\theta_S$  is

$$\langle (\Delta Q_S)^2 \rangle = \frac{1}{4}\{1 + \langle : [e^{-i\theta_S}G_{SS}\Delta S(0) + \text{H.c.}]^2 : \rangle + 2|G_{S-}|^2\}, \quad (\text{A2})$$

where we made use of (38). The noise introduced by the spin quanta created in pairs with the Raman luminescence photons is represented by the contribution  $\sim |G_{S-}|^2$ .

In terms of the signal-spin covariance matrix, the correlation between the two subsystems at  $t = T$  is described by

$$\begin{aligned} \frac{1}{2}\langle (\Delta Q_d\Delta Q_S + \Delta Q_S\Delta Q_d) \rangle &= \frac{1}{4}\{ \langle : [e^{-i(\theta_h-\theta_R)}\sqrt{\eta}\Delta S(0) + \text{H.c.}] [e^{-i\theta_S}G_{SS}\Delta S(0) + \text{H.c.}] : \rangle \\ &+ (e^{-i(\theta_h-\theta_S)}G_{d-}G_{S-}^* \langle \Phi_S^{(-)\dagger}\Phi_d^{(-)} \rangle + \text{c.c.}) \}, \end{aligned} \quad (\text{A3})$$

where the commutation relation (39) was used. The retrieved signal and the residual spin are correlated (i) due to a partial transfer of the initial spin quadratures to both the signal and the spin by an incomplete retrieval and (ii) because of parametric two-quantum interaction in the luminescence channel, similar to the case of  $\chi^{(2)}$  nonlinearity. Equation (A3) implies that for the vacuum initial state of the spin, the light-matter correlation is of parametric origin, as it should be.

### APPENDIX B: SELF-CONSISTENCY OF THE APPROACH

It is instructive to reveal to what extent our basic equations (16) and (17) preserve bosonic commutation relations of the observables. The macroscopic increments of the relevant commutators are evaluated by making use of the observables' increments of the form

$$\Delta O(t) = A_O(t)\Delta t + \int_t^{t+\Delta t} dt' F_O(t'),$$

where  $O$  stands for  $\mathcal{E}$  or  $S$ , the slow uniform terms on the right side of (16) and (17) are denoted as  $A_O(t)$ , and  $F_O(t)$  are the noise sources (18) and (19). Here the time increment  $\Delta t$  is much shorter than a macroscopic evolution time but large compared to the noise correlation time. It is straightforward to demonstrate that given  $[\mathcal{E}(t), \mathcal{E}(t)^\dagger] = [S(t), S(t)^\dagger] = 1$ ,  $[S(t), \mathcal{E}(t)^\dagger] = 0$ , the macroscopic increments of the commutators  $[\mathcal{E}, \mathcal{E}^\dagger]$  and  $[S, S^\dagger]$  are equal to zero, as they should, but for the increment of  $[S, S^\dagger]$  we arrive at

$$\frac{\langle \Delta[S, S^\dagger](t) \rangle}{\Delta t} = -\frac{2\gamma_\perp |\Omega(t)|^2}{\Delta^2}.$$

The right side of this equation gives the ground state excitation rate by the off-resonant control field in the luminescence channel. Since the initial population of the ground state is assumed to be unchanged during the evolution, the necessary condition for our theory to be applicable is  $(2\gamma_\perp |\Omega|^2 / \Delta^2)T \ll 1$  when a relative decrease in the ground-state population is negligible.

- 
- [1] K. Hammerer, A. S. Sorensen, and E. S. Polzik, *Rev. Mod. Phys.* **82**, 1041 (2010).
  - [2] J.-L. Le Gouet and S. Moiseev, Special issue on quantum memories, *J. Phys. B: At. Mol. Opt. Phys.* **45**(12), 120201 (2012).
  - [3] F. Bussieres, N. Sangouard, M. Afzelius, H. de Riedmatten, C. Simon, and W. Tittel, *J. Mod. Opt.* **60**, 1519 (2013).
  - [4] K. Heshami, D. G. England, P. C. Humphreys, P. J. Bustard, V. M. Acosta, J. Nunn, and B. J. Sussman, *J. Mod. Opt.* **60**, 2005 (2016).
  - [5] D. V. Vasilyev, I. V. Sokolov, and E. S. Polzik, *Phys. Rev. A* **77**, 020302(R) (2008).
  - [6] R. Chrapkiewicz and W. Wasilewski, *Opt. Express* **20**, 29541 (2012).
  - [7] X. Zhang, A. Kalachev, and O. Kocharovskaya, *Phys. Rev. A* **87**, 013811 (2013).
  - [8] V. Parigi, V. D'Ambrosio, C. Arnold, L. Marrucci, F. Sciarrino, and J. Laurat, *Nat. Commun.* **6**, 7706 (2015).
  - [9] A. N. Vetlugin and I. V. Sokolov, *Europhys. Lett.* **113**, 64005 (2016).
  - [10] P. B. R. Nisbet-Jones, J. Dille, A. Holleccek, O. Barter, and A. Kuhn, *New J. Phys.* **15**, 053007 (2013).
  - [11] X.-H. Bao, A. Reingruber, P. Dietrich, J. Rui, A. Duck, T. Strassel, L. Li, N.-L. Liu, B. Zhao, and J.-W. Pan, *Nat. Phys.* **8**, 517 (2012).
  - [12] E. Bimbard, R. Boddada, N. Vitrant, A. Grankin, V. Parigi, J. Stanojevic, A. Ourjoumtsev, and P. Grangier, *Phys. Rev. Lett.* **112**, 033601 (2014).
  - [13] D. J. Saunders, J. H. D. Munns, T. F. M. Champion, C. Qiu, K. T. Kaczmarek, E. Poem, P. M. Ledingham, I. A. Walmsley, and J. Nunn, *Phys. Rev. Lett.* **116**, 090501 (2016).
  - [14] A. V. Gorshkov, A. Andre, M. D. Lukin, and A. S. Sorensen, *Phys. Rev. A* **76**, 033804 (2007).
  - [15] J. Stanojevic, V. Parigi, E. Bimbard, R. Tualle-Brouri, A. Ourjoumtsev, and P. Grangier, *Phys. Rev. A* **84**, 053830 (2011).
  - [16] N. G. Veselkova and I. V. Sokolov, *Opt. Spectrosc.* **123**, 82 (2017).
  - [17] N. G. Veselkova and I. V. Sokolov, *Laser Phys.* **27**, 125203 (2017).
  - [18] N. Lauk, C. O'Brien, and M. Fleischhauer, *Phys. Rev. A* **88**, 013823 (2013).

- [19] G. Geng, G. T. Campbell, J. Bernu, D. B. Higginbottom, B. M. Sparkes, S. M. Assad, W. P. Zhang, N. P. Robins, P. K. Lam, and B. C. Buchler, [New J. Phys.](#) **16**, 113053 (2014).
- [20] N. Prajapati, G. Romanov, and I. Novikova, [J. Opt. Soc. Am. B](#) **34**, 001994 (2017).
- [21] J. Nunn, J. H. D. Munns, S. Thomas, K. T. Kaczmarek, C. Qiu, A. Feizpour, E. Poem, B. Brecht, D. J. Saunders, P. M. Ledingham, D. V. Reddy, M. G. Raymer, and I. A. Walmsley, [Phys. Rev. A](#) **96**, 012338 (2017).
- [22] J. Dille, P. Nisbet-Jones, B. W. Shore, and A. Kuhn, [Phys. Rev. A](#) **85**, 023834 (2012).